Stress-free layers in photoinduced deformations of photoelastomer beams

Zoltán Ábrahám[a], György Károlyi[b]

[a]*Faculty of Civil Engineering, Budapest University of Technology and Economics, Műegyetem rkp. 3., H-1111 Budapest, Hungary*
[b]*Institute of Nuclear Techniques, Budapest University of Technology and Economics, Műegyetem rkp. 9., H-1111 Budapest, Hungary*

Abstract

Nematic liquid crystals combined with long molecular chains to form liquid crystal elastomers are capable of large extension. When such liquid crystal elastomers contain azo dyes to constitute photoelastomers, illumination can trigger large contraction. Beams made from such photoelastomers possess a non-uniform illumination and hence photostrain across their cross-section, resulting in bending and highly nonlinear stress distribution. Due to the nonlinear stress distribution, there can be more than one stress-free layers within the beam. In this paper, we present a dimensionless parametric study of nematic photoelastomer beams under the combined effects of light and mechanical loads. We show how the number of stress-free layers depends on three dimensionless parameters. The paths traced out by the system in the space of dimensionless parameters by varying the different real parameters are investigated, showing how the number of stress-free layers changes when e.g. the thickness or the mechanical load of the elastomer beam is varied. These results are important if the strain induced director rotation is not negligible.

Keywords:
photoelastomer beam, nematic liquid crystal, bending, nonlinear stress distribution

1. Introduction

Stiff, rod-like molecules constituting nematic liquid crystals align below the nematic-isotropic phase transition temperature, resulting in uniaxial ori-

entational order [1]. When rubber is formed from nematic liquid crystals by including a network of long molecular chains, the resulting liquid crystal elastomer becomes capable of large extension (up to 400 %) when taken through its nematic-isotropic phase transition temperature [1, 2, 3]. When the liquid crystal elastomer contains azo dyes (e.g. azobenzene) or other photoisomerizable molecular rods, under the effect of light, photon absorption implies a trans $\rightarrow$ cis transition and the shape of these rods become strongly kinked [4, 5], see Fig. 1a. This effect dilutes the nematic order and results in the contraction of the liquid crystal elastomer. This contraction of photoelastomers is comparable in magnitude to that observed for thermal nematic-isotropic phase transition [3, 6].

If a beam built from a photoelastomer is illuminated from one side, as in Fig. 1b, light penetrates the beam. However, due to absorption, the distribution of light across the depth of the beam is not uniform, resulting in an uneven photostrain across the beam. This inhomogeneity implies the bending of the beam [7, 8, 9, 10, 11].

In the simplest approximation, according to Beer's law, photon absorption causes light intensity to decay exponentially with the depth of penetration [7]. Since light intensity governs the nematic order, the latter is also not uniform across the thickness of the elastomer beam. As a consequence, a non-uniform photoinduced strain in nematic photoelastomer beams develops, decaying also exponentially with the depth. The induced stress will hence also be nonlinear across the cross-section of the photoelastomer beam, and up to two stress-free layers can develop [7, 8] when the beam is illuminated from one side as in Fig. 1b.

In the more general case, when light intensity is not assumed to decay exponentially with depth, one has to take into account how the trans and cis fractions of the incorporated azo dye vary with depth as a consequence of absorption [8, 9, 10, 11]. In equilibrium, the trans $\rightarrow$ cis transition caused by illumination is balanced by the cis $\rightarrow$ trans back reaction in each layer of the beam. The light intensity at a certain layer is governed by the absorption in the layers towards the illuminated side of the beam. This nonlinear effect causes an even more complex stress distribution across the beam than in the case when Beer's law is valid. As a consequence, up to three stress-free layers can be found across the cross-sections of such beams [8, 10, 11].

In this paper, we offer a systematic dimensionless parametric study of nematic photoelastomer beams under the effects of incoming light and imposed mechanical load (eccentric force). We show analytically how the number of

stress-free layers depends on the dimensionless parameters of the problem. It turns out that the number of stress-free layers depends on three parameters: beside the intensity of the incoming light, two more dimensionless parameters determine the behavior, both of them being complicated functions of the real parameters of the beam, including the mechanical load, the elastic properties, the geometrical parameters and material properties. We also show the paths traced out by the system in the space of dimensionless parameters when the mechanical loads or the characteristic decay length of the illumination are varied. This sheds light on how the number of stress-free layers depends on the parameters. This can be important because there is evidence that the orientational order can depend on whether parts of the beam are in tension or in compression [12]. Hence a more refined theory of bending of photoelastomer beams under incident light should incorporate in a self-consistent way which layers are in tension or in compression, being separated by the stress-free layers investigated in this paper.

2. Illuminated photoelastomer beam

We follow Ref. [8] to derive the strain induced by light and the corresponding strain and stress distribution across the photoelastomer beam. Then we formulate the dimensionless equation governing the number of stress-free layers.

2.1. Light induced strain

When azobenzene absorbs light, it undergoes the trans $\rightarrow$ cis transition. Hence the trans fraction n_t within the sample decays, but at the same time it is increased by the cis $\rightarrow$ trans spontaneous backreactions:

$$\dot{n}_t = -\Gamma I n_t + n_c/\tau, \tag{1}$$

where $n_c = 1 - n_t$ is the cis fraction, Γ is the constant rate of transition assumed to be independent of nematic order, τ is the average lifetime of cis state that gives constant rate of thermal back relaxation, and dot indicates time derivative. The light intensity is denoted by I. Here we ignored [8] the photo-induced cis $\rightarrow$ trans back-reaction [17] and also the effects of temperature change due to illumination. We look for the steady state $\dot{n}_t = 0$, hence we find

$$n_c(x) = \frac{I(x)}{I_c + I(x)}, \quad n_t(x) = \frac{I_c}{I_c + I(x)}, \tag{2}$$

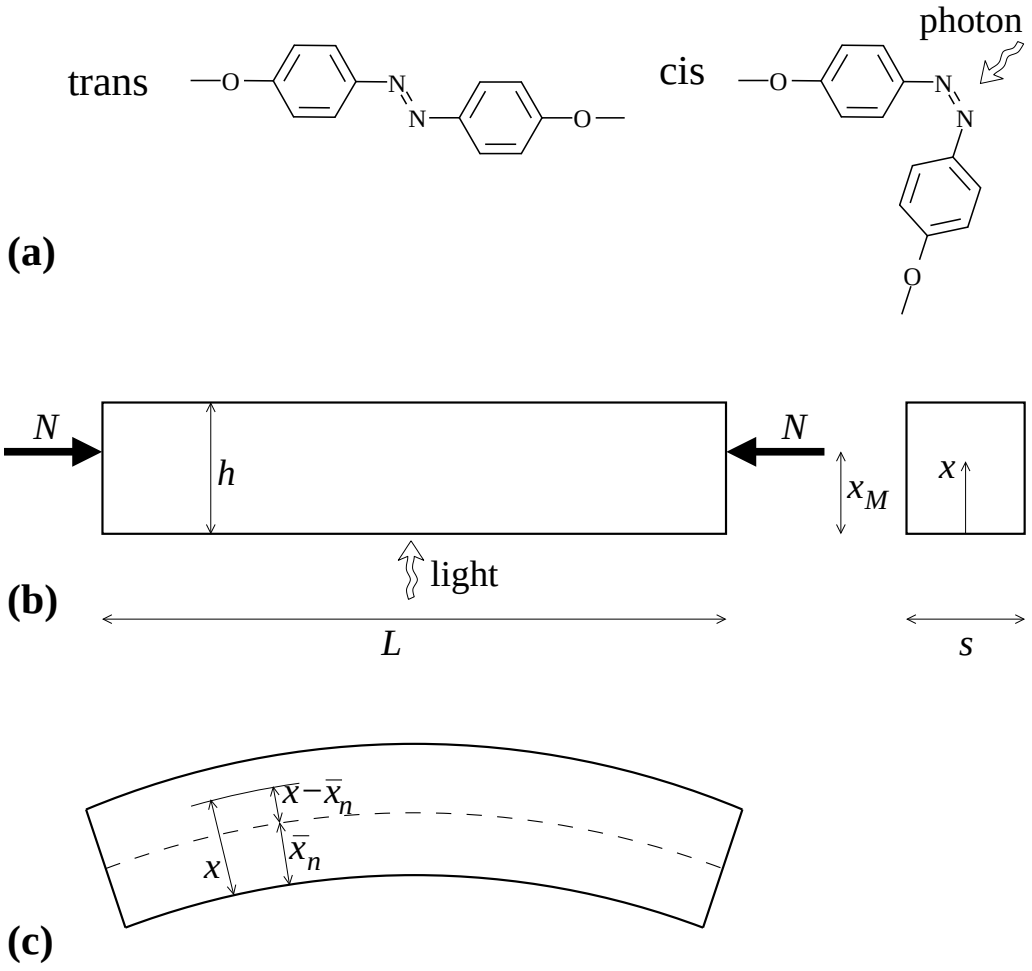

Figure 1: (a) The trans → cis transformation of azobenzene under photon absorption, adapted from Ref. [5]. (b) Layout of the illuminated beam under eccentric load N. (c) Deformed shape with neutral layer at $\overline{x}_n$.

with $I_c = 1/\Gamma\tau$. In steady state the cis and trans fractions and light intensity depend only on depth x measured from the illuminated surface of the beam, see Fig. 1b. Light decays within the material due to absorption as $\mathrm{d}I/\mathrm{d}x = -n_t I/d$, where d is the attenuation length, another material constant. Absorption due to non-dye matrix is ignored for simplicity, it would

only rescale the value of $I(x)$ [9]. Substituting (2) implies

$$\frac{\mathrm{d}I(x)}{\mathrm{d}x} = -\frac{1}{d}\frac{I(x)I_c}{I(x)+I_c}. \tag{3}$$

Integrating this equation with $I(0) = I_0$ (light intensity at the illuminated surface) gives

$$\log\left(\frac{I(x)}{I_0}\right) + \frac{I(x)-I_0}{I_c} = -\frac{x}{d}. \tag{4}$$

In the case when I_c is large ($I_c \gg I_0$), that is, $\Gamma\tau I_0 \ll 1$, we are in the Beer's law regime, when the cis fraction is small, trans fraction is close to one, which is the case when illumination is low. In this special case we find $\log(I(x)/I_0) = -x/d$, i.e., an exponential decay $I(x) = I_0 e^{-x/d}$ of light intensity with depth.

The strain $\varepsilon_r(x)$ imposed by illumination is assumed to be proportional to the cis fraction $n_c(x)$, valid for low azoconcentration (up to 10 wt%) [11]:

$$\varepsilon_r(x) = -An_c(x), \tag{5}$$

where $A > 0$ is a material constant, assumed not to depend on the nematic order. The negative sign is due to the fact that the trans→cis transition implies a strong kink in the azobenzene containing molecules disrupting the nematic order, hence resulting in contraction, see Fig. 1a. Using Eqs. (5), (2) and (3) we find

$$\varepsilon_r(x) = -\frac{AI(x)}{I(x)+I_c} = \frac{Ad}{I_c}\frac{\mathrm{d}I(x)}{\mathrm{d}x}. \tag{6}$$

In the large I_c limit (Beer's law), this simplifies to

$$\varepsilon_r(x) = -\frac{A}{I_c}I(x). \tag{7}$$

This implies that Beer's law is valid in the $I_c \to \infty$, $A \to \infty$ limit as long as A/I_c remains finite.

2.2. Light induced bending

As the photoinduced strain $\varepsilon_r(x)$ depends on depth x, the non-uniform and nonlinear photostrain across the cross-section of the beam leads to bending. Assuming that the cross-sections remain planar, a nonlinear stress distribution $\sigma(x)$ develops across the cross-section implying an elastic strain

$$\varepsilon_b(x) = \sigma(x)/E, \tag{8}$$

where E is Young's modulus of linear elasticity, which is assumed not to depend on the nematic order. The total strain is hence

$$\varepsilon(x) = \varepsilon_b(x) + \varepsilon_r(x). \tag{9}$$

With a stress-free surface at $x = x_n$, i.e., $\sigma(x_n) = 0$, we find $\varepsilon_b(x_n) = 0$ and hence $\varepsilon(x_n) = \varepsilon_r(x_n)$. Similarly, with a strain-free neutral surface at $\overline{x}_n$, i.e., $\varepsilon(\overline{x}_n) = 0$, we can assume that the cross-sections rotate around the $x = \overline{x}_n$ axis with a curvature κ, and hence

$$\varepsilon(x) = \kappa(x - \overline{x}_n). \tag{10}$$

We can express $\kappa\overline{x}_n$ from (10), and also from (10) after substituting x_n in place of x. Then equating these two we find

$$\varepsilon_b(x) + \varepsilon_r(x) = \varepsilon(x) = \varepsilon(x_n) + \kappa(x - x_n) = \varepsilon_r(x_n) + \kappa(x - x_n). \tag{11}$$

This leads to the geometrical equation

$$\varepsilon_b(x) = \kappa(x - x_n) + \varepsilon_r(x_n) - \varepsilon_r(x). \tag{12}$$

Substituting this into the material equation

$$\sigma(x) = E\varepsilon_b(x), \tag{13}$$

then into the equations expressing the balance of stresses and external normal force N and moment Nx_M acing on the cross-section (see Fig. 1b):

$$\int\limits_{(A)} \sigma(x)\mathrm{d}A = N, \quad \int\limits_{(A)} x\sigma(x)\mathrm{d}A = Nx_M, \tag{14}$$

we can integrate (14). We find

$$\begin{aligned} \frac{N}{Es} + \int\limits_0^h \varepsilon_r(x)\mathrm{d}x - h\varepsilon_r(x_n) &= \kappa\left(\frac{h^2}{2} - x_n h\right), \\ \frac{Nx_M}{Es} + \int\limits_0^h x\varepsilon_r(x)\mathrm{d}x - \frac{h^2}{2}\varepsilon_r(x_n) &= \kappa\left(\frac{h^3}{3} - x_n\frac{h^2}{2}\right), \end{aligned} \tag{15}$$

where s is the width, h is the height of the beam, see Fig. 1b. The actual form of $\varepsilon_r(x)$ can be substituted from (6), leading to

$$\begin{aligned}
\int_0^h \varepsilon_r(x)\mathrm{d}x &= \frac{Ad}{I_c}\int_0^h \frac{\mathrm{d}I}{\mathrm{d}x}\mathrm{d}x = \frac{Ad}{I_c}(I_h - I_0), \\
\int_0^h x\varepsilon_r(x)\mathrm{d}x &= \frac{Ad}{I_c}\int_0^h x\frac{\mathrm{d}I}{\mathrm{d}x}\mathrm{d}x = \frac{Adh}{I_c}I_h + \frac{Ad^2}{2I_c^2}(I_h^2 - I_0^2) + \\
&\quad \frac{Ad^2}{I_c}(I_h - I_0), \qquad (16)
\end{aligned}$$

where $I_h = I(h)$ is the intensity of light at the backside of the beam, which is determined by (4).

Putting these back into (15) and dividing the second equation of (15) by the first we can get rid of the curvature κ, and obtain an equation with x_n, the location of the stress-free surface, as the only unknown:

$$\begin{aligned}
\varepsilon_r(x_n) + x_n\Bigg[&-\frac{12Nx_M}{Esh^3} + \frac{6N}{Esh^2} \quad + \\
&\frac{6AdI_0}{h^3I_c}\left(-h\frac{I_h}{I_0} - h - \frac{dI_h^2}{I_cI_0} + d\frac{I_0}{I_c} - \frac{2dI_h}{I_0} + 2d\right)\Bigg] \quad + \\
&\Bigg[\frac{6Nx_M}{Esh^2} - \frac{4N}{Esh} \quad + \\
&\frac{AdI_0}{h^2I_c}\left(2h\frac{I_h}{I_0} + 4h + 3d\frac{I_h^2}{I_0I_c} - 3d\frac{I_0}{I_c} + 6d\frac{I_h}{I_0} - 6d\right)\Bigg] \quad = \quad 0. \qquad (17)
\end{aligned}$$

2.3. Dimensionless form

We can cast the equations for the photostrain and the bending into dimensionless form. Let us use d as the length unit and introduce $\xi = x/d$, and let us measure the light intensity in terms of the incident light intensity as $J(\xi) = I(x)/I_0$. We measure the strain in terms of AI_0/I_c, related to the strain on the surface exposed to light so that $e(\xi) = \varepsilon_r(x)I_c/AI_0 = \varepsilon_r(x)/A\alpha$ where $\alpha = I_0/I_c$ measures the strength of illumination. With $\alpha \to 0$ we expect to find Beer's law of exponential decay of illumination with depth.

These dimensionless forms turn (6) into

$$e(\xi) = -\frac{J(\xi)}{\alpha J(\xi) + 1} = \frac{\mathrm{d}J(\xi)}{\mathrm{d}\xi}, \qquad (18)$$

which is solved by

$$\log J(\xi) + \alpha[J(\xi) - 1] = -\xi, \tag{19}$$

if $J(0) = 1$ is used. With $\alpha \to 0$ we indeed find the exponential decay $J(\xi) = e^{-\xi}$ according to Beer's law. In case of nonzero α, (19) is solved in terms of the Lambert W-function $W(z)$ [13]

$$J(\xi) = \frac{1}{\alpha} W(\alpha e^{\alpha - \xi}). \tag{20}$$

Equation (17) can also be cast into the dimensionless form

$$e(\xi_n) + P\xi_n + Q = 0 \tag{21}$$

with $\xi_n = x_n/d$ and

$$\begin{aligned} P &= -\frac{12Nx_M dI_c}{Esh^3 AI_0} + \frac{6NdI_c}{Esh^2 AI_0} + \\ &\quad \frac{6d^2}{h^3}\left(-h\frac{I_h}{I_0} - h - \frac{dI_h^2}{I_c I_0} + d\frac{I_0}{I_c} - \frac{2dI_h}{I_0} + 2d\right), \\ Q &= \frac{6Nx_M I_c}{Esh^2 AI_0} - \frac{4NI_c}{EshAI_0} + \\ &\quad \frac{d}{h^2}\left(2h\frac{I_h}{I_0} + 4h + 3d\frac{I_h^2}{I_0 I_c} - 3d\frac{I_0}{I_c} + 6d\frac{I_h}{I_0} - 6d\right). \end{aligned} \tag{22}$$

Here P and Q are dimensionless parameters that depend on the original parameters of the problem. The number of stress-free layers within the beam, i.e., the number of solutions of (21), are determined by P, Q, and also by α which enters (21) through the actual form of $e(\xi)$, see (18) and (19).

3. Number of stress-free layers

3.1. Properties of the intensity and strain functions

Since $J(\xi)$ was defined as $J(\xi) = I(x)/I_0$, we see that $J(0) = 1$. Physically, light intensity $J(\xi)$ cannot be negative, so we only investigate here this case (the $J < 0$ case possesses a graph separated from the one obtained below for $J \geq 0$). For $J > 0$, from (18) we find that $\mathrm{d}J(\xi)/\mathrm{d}\xi < 0$ hence $J(\xi)$ decreases monotonously, and it has zero slope for $J = 0$ only.

From (19) we find that $\lim_{\xi\to-\infty} J(\xi) = \infty$ and $\lim_{\xi\to\infty} J(\xi) = 0$. Also, taking the derivative of (18) with respect to ξ we find

$$\frac{\mathrm{d}^2 J(\xi)}{\mathrm{d}\xi^2} = \frac{J(\xi)}{[1+\alpha J(\xi)]^3}, \tag{23}$$

hence $\mathrm{d}^2 J(\xi)/\mathrm{d}\xi^2 > 0$ if $J > 0$, which means that the curvature does not change sign. Also, from (18) we find that $\lim_{\xi\to-\infty} \mathrm{d}J(\xi)/\mathrm{d}\xi = -1/\alpha$ and $\lim_{\xi\to\infty} \mathrm{d}J(\xi)/\mathrm{d}\xi = 0$. Based on these observations, the graph of $J(\xi)$ is shown in Fig. 2a for several values of α, the strength of incident illumination.

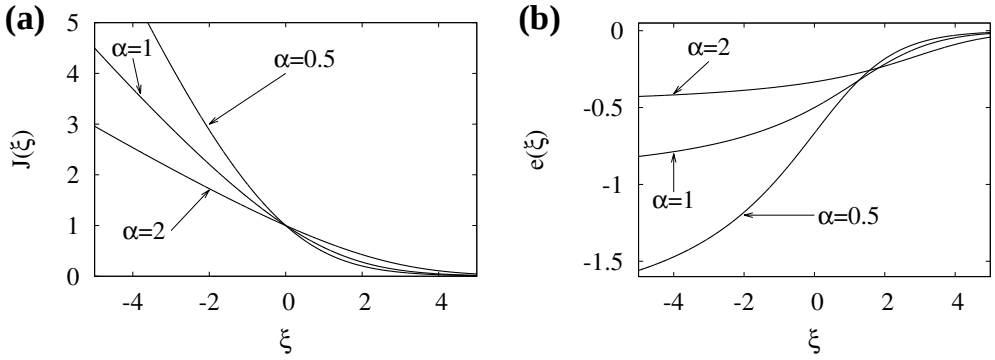

Figure 2: Graphs of (a) $J(\xi)$ and (b) $e(\xi)$ for several values of α. The slope of $J(\xi)$ and hence the value of $e(\xi) = \mathrm{d}J(\xi)/\mathrm{d}\xi$ asymptotes to $-1/\alpha$ for $\xi \to \infty$, and to 0 for $\xi \to \infty$.

We can also draw the graph of the photostrain $e(\xi) = \mathrm{d}J(\xi)/\mathrm{d}\xi$. We have seen that for $J \geq 0$, $\mathrm{d}J(\xi)/\mathrm{d}\xi = e(\xi) \leq 0$. Having already obtained the limiting cases for the derivatives of $J(\xi)$, we have $\lim_{\xi\to-\infty} e(\xi) = -1/\alpha$ and $\lim_{\xi\to\infty} e(\xi) = 0$. To find the zero slope of $e(\xi)$, we need to find where the second derivative of $J(\xi)$ is zero: from (23) we see that it is either at $J \to 0$ implying $\xi \to \infty$ or at $J \to \pm\infty$ implying $\xi \to -\infty$. It is also easy to verify that $e(0) = -1/(1+\alpha)$. Based on these observations, the graph of $e(\xi)$ is shown in Fig. 2b for several values of α.

Note that in the special case $\alpha \to 0$ (Beer's law) both Fig. 2a and b are simple exponential functions, which implies a dramatic change in Fig. 2b: it decreases unbounded for $\xi \to -\infty$, whereas for $\alpha > 0$ it is bounded from below as it asymptotes to $-1/\alpha$.

3.2. Number of stress-free layers

In order to find stress-free layers, we need to look for intersections of the graph of $e(\xi)$ with the line $-P\xi - Q$, see (21) and Fig. 2b.

In case $P > 0$, there is always one intersection of $e(\xi)$ with $-P\xi - Q$, and hence there is always one stress-free layer. This unique stress-free layer is within the cross-section of the beam if the intersection falls in the interval $\xi \in [0, h/d]$, which occurs if

$$\frac{J_h}{1+\alpha J_h} - \frac{h}{d}P \leq Q \leq \frac{1}{1+\alpha}, \tag{24}$$

where $J_h = J(h/d)$ is dimensionless backside light intensity.

In case $P = 0$, there can be zero or one stress-free layer. If

$$0 \leq Q \leq 1/\alpha \tag{25}$$

there is one, otherwise there is zero stress-free layer. Moreover, if

$$\frac{J_h}{1+\alpha J_h} \leq Q \leq \frac{1}{1+\alpha}, \tag{26}$$

the single stress-free layer falls within the cross-section of the beam.

The most interesting case is the $P < 0$ case: the number of intersections of $e(\xi)$ with $-P\xi - Q$ can be 1, 2 or 3 for $\alpha > 0$. The case of 1 or 3 intersections is separated by the case of 2 solutions, where the two curves [$e(\xi)$ and $-P\xi - Q$] touch each other with the same tangent. So first we look for such tangential cases. In this case, not only (21) has to be fulfilled, but $\mathrm{d}e(\xi)/\mathrm{d}\xi = -P$ must also hold, which, through (18) implies

$$\frac{J}{(1+\alpha J)^3} = -P. \tag{27}$$

We can substitute (18) and (19) into (21) so that it only contains J:

$$\frac{J}{1+\alpha J} = Q - P\log(J) - P\alpha(J-1). \tag{28}$$

Once (27) is solved for J, it can be substituted into (28) to find the relation for exactly two stress-free layers in terms of P, Q and α.

Equation (27) is a third-order equation

$$\alpha^3 J^3 + 3\alpha^2 J^2 + (3\alpha + 1/P)J + 1 = 0 \tag{29}$$

with discriminant

$$\Delta = \frac{1}{\alpha^8 P^2}\left(\frac{1}{4} + \frac{1}{27\alpha P}\right). \tag{30}$$

The sign of the discriminant determines the number of real solutions.

If $P < -4/27\alpha$ (implying $\Delta > 0$) there is one real solution for J, which turns out to be negative, hence unphysical, since J must be positive.

If $P = -4/27\alpha$ (implying $\Delta = 0$) there are three real solutions two of which coincide. The single root is negative and hence unphysical, the two coinciding roots are $1/2\alpha$. Writing it back into (28), with $P = -4/27\alpha$, gives

$$P = -\frac{4}{27\alpha}, \quad Q = \frac{4}{27} + \frac{7}{27\alpha} + \frac{4\log(2\alpha)}{27\alpha} \tag{31}$$

as the condition for having two stress-free layers.

If $P > -4/27\alpha$ (implying $\Delta < 0$) there are three different real roots. One of them is always negative (unphysical), the other two are positive:

$$J = -\frac{1}{\alpha} - \frac{1}{\alpha}\frac{2}{\sqrt{-3\alpha P}}\cos\left[\frac{2\pi}{3} \pm \frac{1}{3}\arccos\left(\sqrt{-\frac{27}{4}\alpha P}\right)\right]. \tag{32}$$

These solutions, substituted into (28), define curves in the (P, Q) plane along which the number of stress-free surfaces is two. We note that the two curves end in the point defined by (31) obtained for $P = -4/27\alpha$.

Based on these results, Fig. 3 shows the regions with various number of stress-free layers, for several values of α. We can see that there is a region where the number of stress-free layers is three, that is, there are two layers in tension and two layers in compression across the cross-section. We see that with the decrease of α the region with three stress-free layers expands. The curve defined using the negative sign in (32) goes further from the origin as α is decreased, and disappears for $\alpha \to 0$. The curve defined by the positive sign in (32) converges to the curve

$$Q = -P[1 - \log(-P)] \tag{33}$$

as $\alpha \to 0$, which separates the regions with zero or 2 stress-free layers, and is valid in case Beer's law is valid, see Fig. 4.

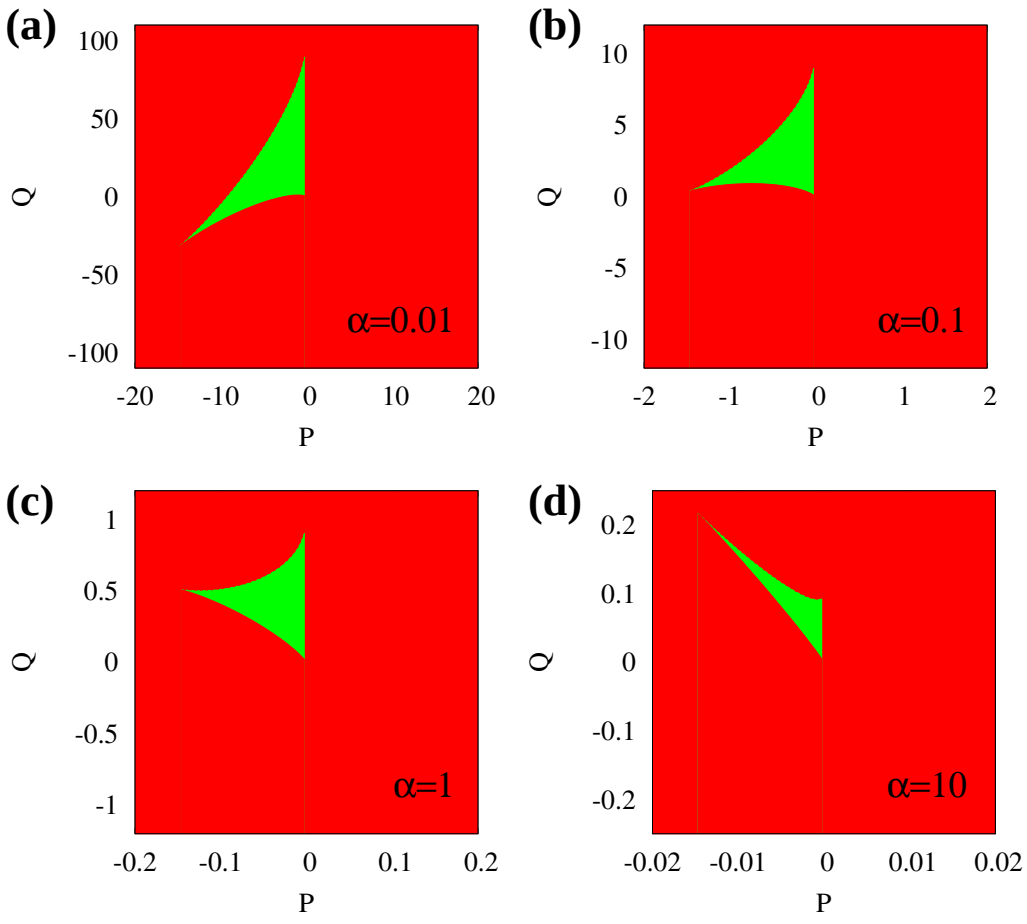

Figure 3: Regions colour coded according to the number of stress-free layers for various values of incident illumination α in the (P, Q) plane. Red indicates 1, green 3 stress-free layers. There are 2 stress-free layers for values of $P < 0$ and Q that fall on the boundary between the red and green regions. Note the different scales on the axes.

3.3. Variation of parameters

Figure 3 shows the number of stress-free layers as P or Q are varied. One can ask how the number of stress-free layers changes as the original parameters are varied. One can rewrite Eqs. (22) in terms of more meaningful, but still dimensionless parameters. Let us introduce $\beta = AI_0/I_c$ [remains finite when $\alpha = I_0/I_c \to 0$, see after Eq. (7)], $\delta = h/d$ (height of beam relative to attenuation length), $n = N/Esh\beta$ (rescaled normal force) and $m = x_M/h$

(relative position of the normal force, $m = 0.5$ means no eccentricity). Using these dimensionless parameters, (22) can be rewritten as

$$P = \frac{6\delta^2 n(1-2m) - 6\delta(1+J_h) + 6\alpha(1-J_h^2) + 12(1-J_h)}{\delta^3},$$
$$Q = \frac{\delta^2 n(6m-4) + 2\delta(2+J_h) + 3\alpha(J_h^2-1) + 6(J_h-1)}{\delta^2}. \tag{34}$$

Using these formulas, in principle, one can draw curves on the (P, Q) plane by varying one of the parameters δ, m or n to see how the change of that parameter affects the number of stress-free layers. In the general, $\alpha \neq 0$ case, the illumination J_h on the backside of the beam can be given from (20) as $J_h = W(\alpha e^{\alpha-\delta})/\alpha$.

In the Beer's law case ($\alpha \to 0$), due to $J_h = e^{-\delta}$, (34) reduces to

$$P = \frac{6\delta^2 n(1-2m) - 6\delta(1+e^{-\delta}) + 12(1-e^{-\delta})}{\delta^3},$$
$$Q = \frac{\delta^2 n(6m-4) + 2\delta(2+e^{-\delta}) + 6(e^{-\delta}-1)}{\delta^2}. \tag{35}$$

In Fig. 4, for various values of eccentricity m and normal force n we show how the number of stress-free layers changes as $\delta \geq 0$ is varied. The white curves, parameterized by δ, show how in each case the values of P and Q change when δ is varied. Varying δ, the curves may or may not cross the regions with different number of stress-free layers. When the normal force is tensile ($n \leq 0$), there are 2 stress-free layers for $m \leq 0.5$, and depending on δ there are either one or two stress-free layers for $m > 0.5$. In case of compressive normal force ($n > 0$), depending on the eccentricity m and beam thickness δ, there can be 0, 1 or 2 stress-free layers.

In the general case $\alpha \neq 0$, instead of δ, we parameterize the curves in the (P, Q) plane by J_h. Using (19) with $\xi = \delta$ we can express δ with J_h as $\delta = \alpha(1 - J_h) - \log J_h$. Then using this in (34) δ can eliminated, and we have the parametric curve $(P(J_h), Q(J_h))$ for all fixed values of m and n. As an illustration, the graphs for various values of n and m are shown in Fig. 5 in case of $\alpha = 0.1$. As the region with three stress-free layers is bounded, most of the white curves, parameterized by J_h, lie in the red region with one stress-free layer. However, we can see that for all values of eccentricity m, there are values for the load n and backside illumination (and hence δ) where the number of stress-free layers is three and the white curves pass through the green regions in Fig. 5.

4. Conclusions

In this paper, we presented a dimensionless parametric study of the stress-free layers of photoelastomer beams under the combined effect of illumination and eccentric force. We handled in parallel the cases of low illumination level (Beer's law) and the general case when the variation of the trans and cis fractions within the beam has to be considered. For both cases we found analytic results for the number of stress-free layers. We showed that the number of stress-free layers depends on three dimensionless parameters even in the case of eccentric normal force. It was also investigated how the number of stress-free layers varies as the normal force, its eccentricity and either the attenuation length or the backside illumination change. This is important information when one wishes to consider the strain induced director rotation within the beam [12]. However, in order to use our results in the investigation of strain induced director rotation, the position of the stress-free layers has to be computed as well. In particular, in some cases the number of stress-free layers that fall within the cross-section of the beam can be smaller than the number computed here: some stress-free layers may actually be outside the cross-section. The treatment of this problem requires further work.

During the derivation, we made several simplifying assumptions. We neglected the in-plane contraction due to illumination, which would cause the beam to become thicker; we expect this to have only secondary effect for beams. Also, in case of films a saddle-like shape would occur [18, 19] which can be safely neglected for beams. We assume that the deflection is small or the illumination is caused by diffuse light, otherwise, in case of unidirectional illumination, a significant curvature would imply that the intensity of light falling on the surface would change along the beam.

Besides the theoretical interest in photoelastomer materials we have to point out that these materials are potentially very important in a number of applications. These applications include micropumps [14] or other microfluidic devices [8, 15], photomechanical actuators [8, 16], manipulators of nanostructures [15], and artificial muscles [16]. A recent result in this direction is a simple, light-driven plastic motor [20] in which a laminated photoelastomer belt, illuminated by UV light, drives two pulleys. This is an efficient device to convert light energy into mechanical work.

Acknowledgement

Financial support from OTKA grant No. K 100894 is gratefully acknowledged. We thank for the useful comments of A. Kocsis and A. Bibó, and of the reviewers.

[1] M. Warner, E.M. Terentjev: *Liquid crystal elastomers*. Oxford University Press, Oxford, 2003.

[2] H. Finkelmann, H. Wermter: LC-elastomers and artificial muscles. Abstract of Papers of the American Chemical Society **219** (2000) U493.

[3] A.R. Tajbakhsh, E.M. Terentjev: Spontaneous thermal expansion of nematic elastomers. The European Physical Journal E **6** (2001) 181–188.

[4] C.D. Eisenbach: Isomerization of aromatic azo chromophores in poly(ethyl acrylate) networks and photomechanical effect. Polymer **21** (1980) 1175–1179.

[5] J. Cviklinski, A.R. Tajbakhsh, E.M. Terentjev: UV isomerisation in nematic elastomers as a route to photo-mechanical transducer. The European Physical Journal E **9** (2002) 427–434.

[6] H. Finkelmann, E. Nishikawa, G.G. Pereira, M. Warner: A new opto-mechanical effect in solids. Physical Review Letters **87** (2001) 015501.

[7] M. Warner, L. Mahadevan: Photoinduced deformations of beams, plates, and films. Physical Review Letters **92** (2004) 134302.

[8] D. Corbett, M. Warner: Linear and nonlinear photoinduced deformations of cantilevers. Physical Review Letters **99** (2007) 174302.

[9] D. Corbett, C.L. van Oosten, M. Warner: Nonlinear dynamics of optical absorption of intense beams. Physical Review A **78** (2008) 013823.

[10] D. Corbett, M. Warner: Changing liquid crystal elastomer ordering with light — A route to opto-mechanically responsive materials. Liquid Crystals **36** (2009) 1263–1280.

[11] C.L. van Oosten, D. Corbett, D.Davies, M. Warner, C.W.M. Bastiaansen, D.J. Broer: Bending dynamics and directionality reversal in liquid crystal network photoactuators. Macromolecules **41** (2008) 8592–8596.

[12] D. Corbett, M. Warner: Nonlinear photoresponse of disordered elastomers. Physical Review Letters **96** (2006) 237802.

[13] R.M. Corless, G.H. Gonnet, D.E.G. Hare, D.J. Jeffrey, D.E. Knuth: On the Lambert W function. Advances in Computational Mathematics **5** (1996) 329–359.

[14] M. Chen, X. Xing, Z. Liu, Y. Zhu, H. Liu, Y. Yu, F. Cheng: Photodeformable polymer material: towards light-driven micropump applications. Applied Physics A **100** (2010) 39–43.

[15] Z.Y. Wei, L.H. He: Surface topography and its transition of nematic elastomers due to photoinduced deformation. The Journal of Chemical Physics **124** (2006) 064708.

[16] M.L. Dunn: Photomechanics of mono- and polydomain liquid crystal elastomer films. Journal of Applied Physics **102** (2007) 013506.

[17] D. Corbett, M. Warner: Bleaching and stimulated recovery of dyes and of photocantilevers. Physical Review E **77** (2008) 051710.

[18] M. Camacho-Lopez, H. Finkelmann, P. Palffy-Muhoray, M. Shelley: Fast liquid-crystal elastomer swims into the dark. Nature Materials **3** (2004) 307–310.

[19] M.L. Dunn, K. Maute: Photomechanics of blanket and patterned liquid crystal elastomer films. Mechanics of Materials **41** (2009) 1083–1089.

[20] M. Yamada, M. Kondo, J. Mamiya, Y. Yu, M. Kinoshita, C.J. Barrett, T. Ikeda: Photomobile polymer materials: Towards light-driven plastic motors. Angewandte Chemie (International edition in English) **47** (2008) 4986–4988.

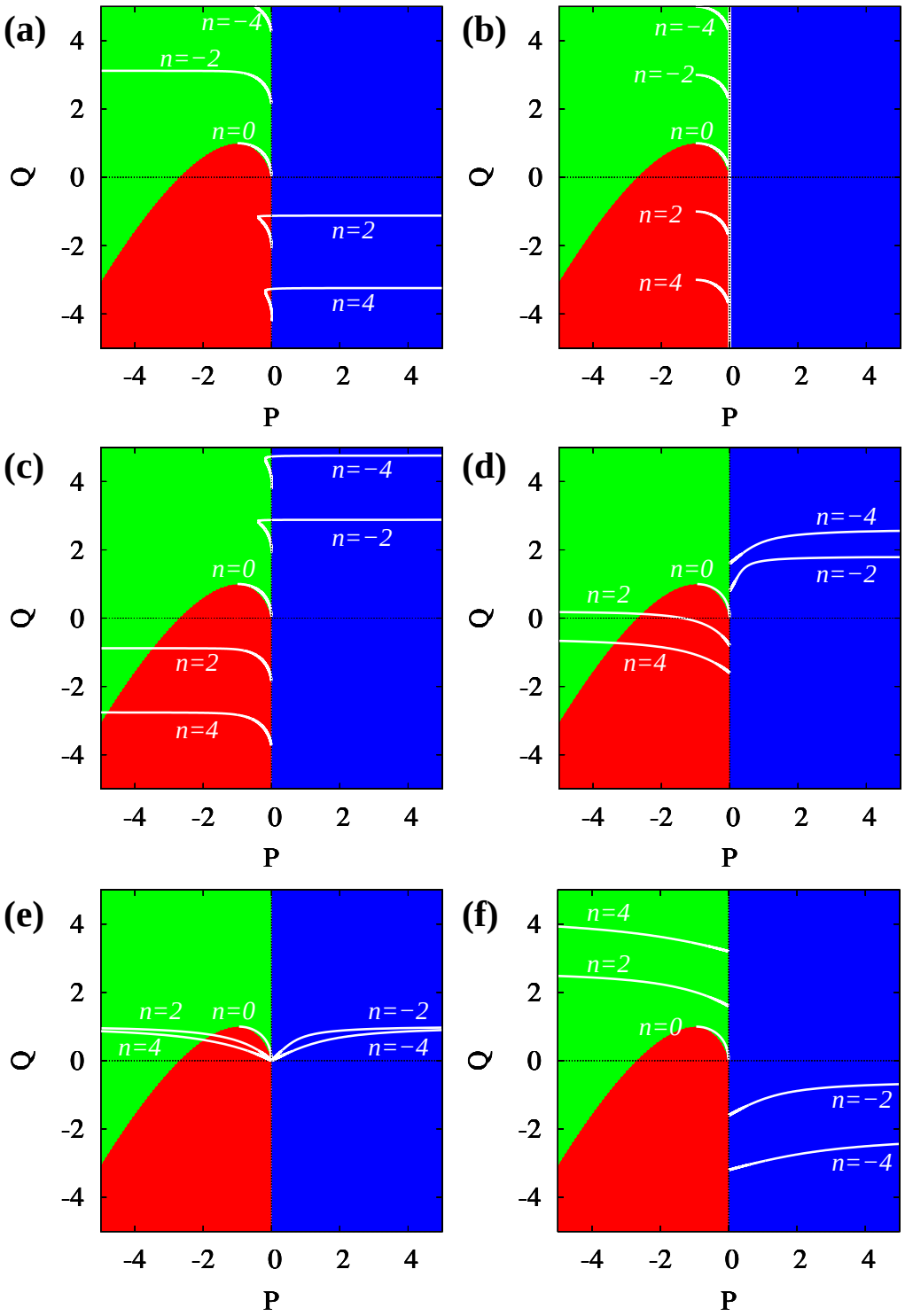

Figure 4: Regions colour coded according to the number of stress-free layers for $\alpha = 0$ (Beer's law) in the (P, Q) plane. Red indicates 0, blue 1 and green 2 stress-free layers. For various values of the magnitude n and eccentricity m of the load [(a) $m = 0.49$, (b) $m = 0.5$, (c) $m = 0.51$, (d) $m = 0.6$, (e) $m = 0.67$ and (f) $m = 0.8$], white curves show how the values of P and Q, and the number of stress-free layers change as the dimensionless attenuation length $\delta > 0$ changes. Note that $n > 0$ implies compressive force and $m = 0.5$ is the case of centric loading.

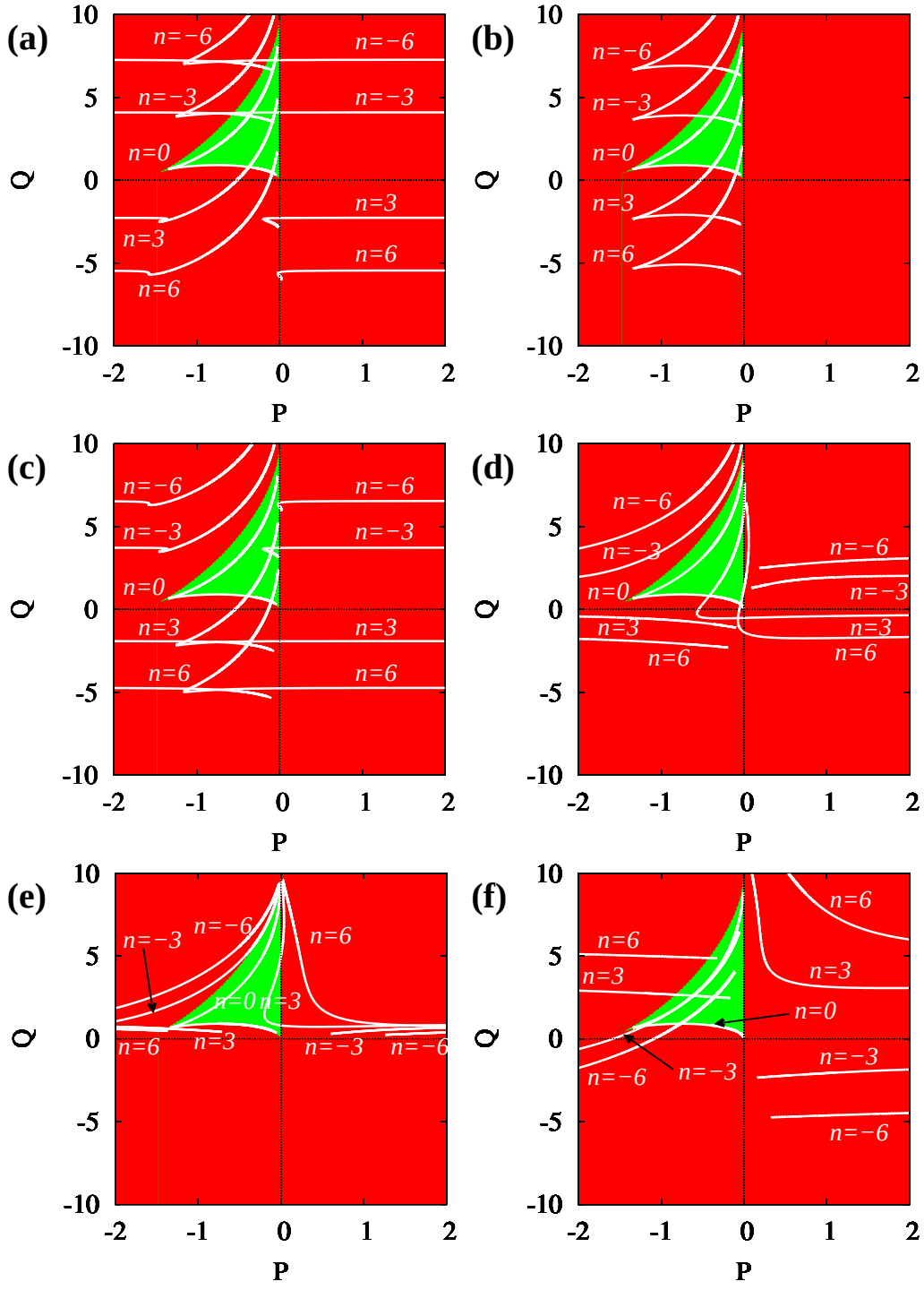

Figure 5: Regions colour coded according to the number of stress-free layers for $\alpha = 0.1$ in the (P, Q) plane. Red indicates 1, green 3 stress-free layers. For various values of the magnitude n and eccentricity m of the load [(a) $m = 0.49$, (b) $m = 0.5$, (c) $m = 0.51$, (d) $m = 0.6$, (e) $m = 0.67$ and (f) $m = 0.8$], white curves show how the values of P and Q, and the number of stress-free layers change as the dimensionless backside light intensity $J_h > 0$ changes. Note that $n > 0$ implies compressive force and $m = 0.5$ is the case of centric loading.